Pushing the Envelope of *In Situ* Transmission Electron Microscopy

Rajaprakash Ramachandramoorthy,[†,‡] Rodrigo Bernal,[†] and Horacio D. Espinosa[*,†,‡]

[†]Department of Mechanical Engineering, Northwestern University, Evanston, Illinois 60208, United States and [‡]Department of Theoretical and Applied Mechanics, Northwestern University, Evanston, Illinois 60208, United States

ABSTRACT

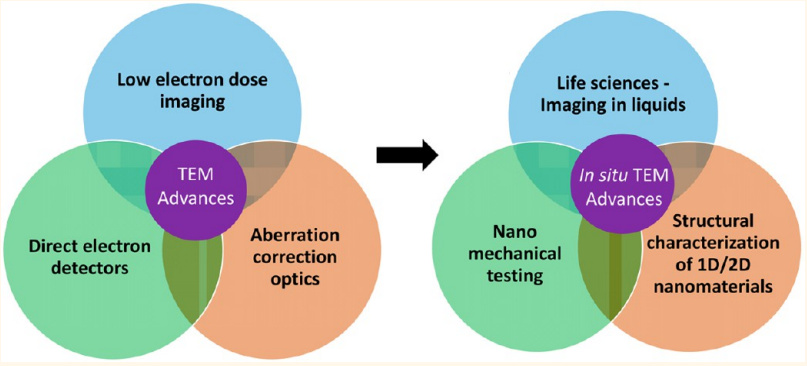

Recent major improvements to the transmission electron microscope (TEM) including aberration-corrected electron optics, light-element-sensitive analytical instrumentation, sample environmental control, and high-speed and sensitive direct electron detectors are becoming more widely available. When these advances are combined with *in situ* TEM tools, such as multimodal testing based on microelectromechanical systems, key measurements and insights on nanoscale material phenomena become possible. In particular, these advances enable metrology that allows for unprecedented correlation to quantum mechanics and the predictions of atomistic models. In this Perspective, we provide a summary of recent *in situ* TEM research that has leveraged these new TEM capabilities as well as an outlook of the opportunities that exist in the different areas of *in situ* TEM experimentation. Although these advances have improved the spatial and temporal resolution of TEM, a critical analysis of the various *in situ* TEM fields reveals that further progress is needed to achieve the full potential of the technology.

Since the invention of the transmission electron microscope (TEM) in 1931 by Max Knoll and Ernst Ruska,[1] the scientific community has been striving to attain the theoretically predicted resolution limit of a 200 kV electron microscope, on the order of ~3 pm.[2] In the last few decades, there have been steady advances in the stability of electron sources and power supplies, improvement in measurement of aberrations, and superior corrector designs. These advances have yielded an increase in resolution from 50 nm to sub-angstrom (0.5 Å),[3] which was recently achieved using a spherical and chromatic aberration-corrected TEM (Cs/Cc-TEM).[4,5]

Furthermore, in the past decade, many sophisticated additions have been brought to TEM, namely, microanalysis tools such as the ChemiSTEM technology, which uses four silicon drift detectors placed close to the sample to conduct energy-dispersive X-ray analysis (EDX) that enables light element detection;[6] the X-field emission gun (X-FEG), which is a Schottky-based high brightness electron source that makes atomic resolution imaging at low electron dose possible;[7] and unique imaging modes such as high-angle annular dark-field (HAADF) based on Rutherford scattering, which permits three-dimensional nano-structural analysis.[8]

A key hurdle in conducting a multitude of *in situ* TEM experiments has been the limited space in the TEM chamber and the associated difficulty in the miniaturization of experimental setups. Historically, in order to obtain high-resolution TEM images, a small pole piece gap of ~2–3 mm is usually required, but with the invention of

* Address correspondence to espinosa@northwestern.edu.

Published online May 05, 2015
10.1021/acsnano.5b01391

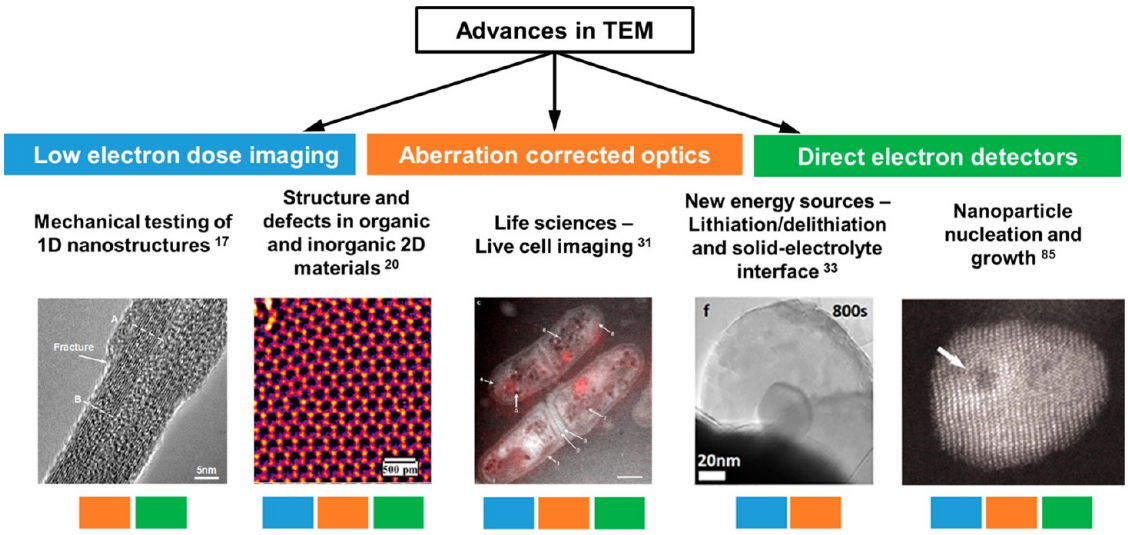

Figure 1. Advances in transmission electron microscopy and its benefits to different *in situ* studies discussed in this Perspective. Images from left to right: Reprinted with permission from ref 17. Copyright 2008 Nature Publishing Group. Reprinted with permission from ref 20. Copyright 2012 American Association for the Advancement of Science. Reprinted with permission from ref 31. Copyright 2011 Elsevier. Reprinted with permission from ref 33. Copyright 2014 Nature Publishing Group. Reprinted with permission from ref 85. Copyright 2012 American Association for the Advancement of Science.

aberration-corrected TEM optics, high-resolution images can be obtained with a larger pole piece gap of ~5 mm.[9] With the advent of microelectromechanical systems (MEMS) and liquid cell technologies, miniaturization of various experiments has become possible.[10−12] These advances have paved the way for multimodal probing of many different nanomaterials and the understanding of their structure and response to various stimuli (see Figure 1).

Some examples of *in situ* TEM research areas that have leveraged these capabilities and advances in TEM include the following: (i) mechanical and electromechanical testing of nanostructures,[13−15] which requires the identification of the crystallographic structure and defects of the testing sample before, during, and after the test in order to correlate the structure and mechanical behavior of the material;[16−18] (ii) capturing dynamic processes in liquids, such as the study of nanoparticle growth mechanisms and trajectories that require *in situ* TEM fitted with closed cells capable of introducing liquids in the high vacuum of TEM;[19] and (iii) imaging of two-dimensional (2D) materials to reveal the atomic structure of defects and their dynamics, which are critical to the discovery of new phenomena (*e.g.*, atomic deformations and interlayer shear interactions).[20,21]

Although developments in TEM, such as aberration correction and energy filtering, and high-speed imaging and acquisition are becoming more widely available, *in situ* experiments have not yet fully leveraged these capabilities. Beyond existing work, including pioneering investigations on mechanical and electromechanical testing of one-dimensional (1D) materials,[15,17,18,22−26] physical/chemical/bio processes in liquid,[27−33] and 2D material structural and defect characterization,[20,34,35] there are enormous opportunities for utilizing the capabilities of *in situ* TEM experimentation. In this Perspective, we provide a snapshot of the state-of-the-art techniques and highlight areas ripe for innovation, while noting remaining challenges.

Mechanical Testing of One-Dimensional Materials. One-dimensional nanomaterials such as carbon nanotubes (CNTs) and nanowires are envisioned in next-generation technologies, including nanoelectromechanical systems for resonators,[36] logical switches,[37] and flexible electronics such as touch screens.[38] This wide range of applications requires characterization of nanostructures under a variety of external stimuli, such as mechanical, electrical, and thermal input. An extensive range of *in situ* TEM holders and techniques have been developed to apply these stimuli and to record the behavior of nanostructures.[10,39−41] Specifically, a variety of holders and testing methods exist to test nanowires and nanopillars *in situ* (for a review, see ref 10), namely, the classical tensile testing holder with high temperature option, bending and shearing holders, and nanoindentation holders.[41] In particular, Espinosa and co-workers pioneered MEMS technology for *in situ* measurement of force and displacement with simultaneous acquisition of high-resolution images of the atomic structure of test specimens. Electronic

> ***In Situ* TEM plays a key role in the *quantitative* characterization of nanomaterials and direct comparisons to quantum mechanical predictions.**

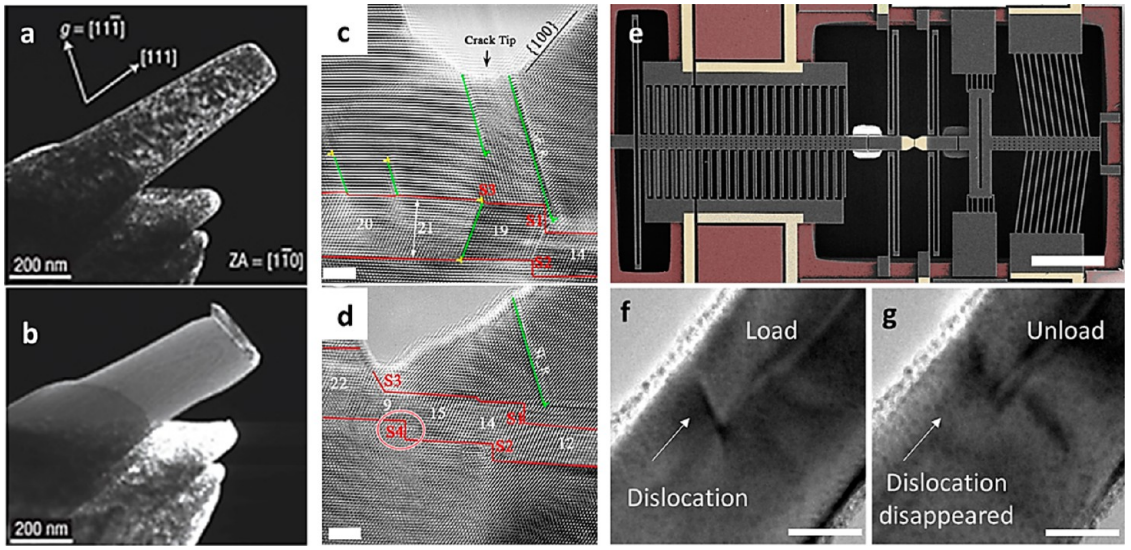

Figure 2. Mechanical annealing in Ni nanopillars (a) before and (b) after compression. Reprinted with permission from ref 40. Copyright 2008 Nature Publishing Group. (c,d) Crack tip propagation in nanotwinned silver (scale bar 2 nm). Reprinted with permission from ref 43. Copyright 2014 Nature Publishing Group. (e) Microelectromechanical system device with displacement control mechanical testing capability (scale bar 300 μm). (f,g) Bauschinger effect in pentatwinned silver nanowires due to reversible dislocation motion (scale bar 20 nm). Reprinted from ref 23. Copyright 2014 American Chemical Society.

actuation and sensing were integrated in a single MEMS device,[14] providing a complete nanoscale testing apparatus in which load is measured with 10 nN resolution and displacement with subnanometer resolution. This made possible the first direct correlation between failure stress and number of failed shells in multiwalled CNTs with excellent agreement to quantum mechanics predictions.[17] Failure modes and carbon atomic structures (intershell cross-linking) were also identified as a function of exposure dose to electron radiation.[17,42] These investigations showed that *in situ* TEM plays a key role in the *quantitative* characterization of nanomaterials and direct comparisons to quantum mechanical predictions.

Despite these advances, monotonic, low-strain-rate testing has dominated the nanomechanics field for the past decade, as shown by the examples of mechanical annealing and crack tip propagation shown in Figure 2a,b[40] and 2c,d.[43] However, an understanding of thermally activated atomistic mechanisms and the fatigue life of nanostructures requires cyclic loading. Recently, Bernal *et al.* made use of MEMS technology, including feedback control, to achieve truly displacement control experiments in tension (Figure 2e).[44] With this platform, recoverable plasticity was observed upon unloading, the magnitude of which can be partial or total depending on the deformation history.[23] *In situ* TEM experiments revealed that this behavior is governed by reversible dislocation activity, as shown in Figure 2f, g, which was investigated in great detail using molecular dynamics (MD) simulations.[23] Similar behavior was observed on load control by studying nanowire stress relaxation.[45] Little work has been carried out toward understanding other time-dependent mechanical behaviors of nanostructures, such as fatigue life estimation.[46−49] However, with the advent of high-speed electron detectors and low-noise MEMS devices, exploring such behavior is in the realm of possibilities.

Another area little pursued in *in situ* TEM studies is the strain rate behavior of nanostructures from 10^{-1}/s to 10^{5}/s. This is primarily due to the lack of testing platforms and limitations in image acquisition. Since nanostructures are likely to be employed in resonators and switches operating at high speeds, understanding their behavior under dynamic conditions is needed for their proper design. Another motivation to conduct high-strain-rate testing at the nanoscale is to validate the different force fields used in MD simulations.[39] However, until now, the results obtained from MD simulations could not be directly compared and validated against the experimental results, due to the significant difference in strain rates between the two approaches. The MD simulations are usually carried out at 10^{6}/s−10^{8}/s, and experiments are usually carried out at quasi-static strain rates at 10^{-4}/s.[22,50] Hence, there is a need to bridge this gap in strain rate either by conducting simulations at lower strain rates or by increasing the strain rates of the experiments. At the mesoscale, high-strain-rate experiments, above 10^{3}/s, are conducted using impact techniques, and the corresponding stress−strain signatures are obtained using interferometric techniques together with analysis.[51,52] At the nanoscale, MEMS-based high-strain-rate tests are possible, but the stress−strain signatures can only be obtained by electrical or high-speed optical sensing. Electrical sensing is feasible, but it involves

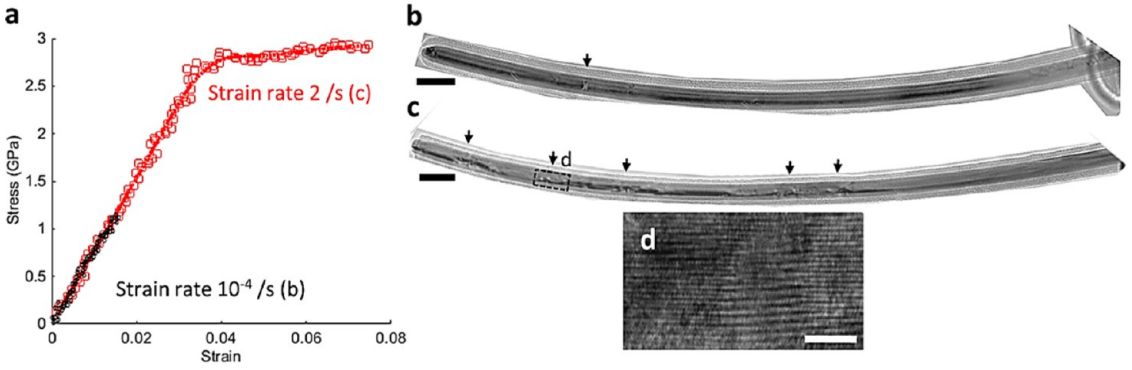

Figure 3. (a) Stress−strain signatures of bicrystalline silver nanowire tested at different strain rates. (b) TEM image of the nanowire tested at a strain rate of 10^{-4}/s, low dislocation density (scale bar 80 nm). (c) TEM image of nanowire tested at strain rate of 2/s, high dislocation density (scale bar 80 nm). (d) Close-up of the dashed square in c) (scale bar 2 nm). Reprinted with permission from ref 54. Copyright 2015 Ramachandramoorthy *et al*.

high-frequency signals that are prone to possible electrical crosstalk[53] and a low signal-to-noise (S/N) ratio. High-speed optical sensing at the nanoscale is difficult to integrate in a TEM.

Recently, we performed multiphysics simulations and conducted a series of calibration tests to understand possible speeds of operation for current MEMS technology. We succeeded in employing previously developed MEMS platforms to conduct nanowire experiments to strain rates up to 2/s. Using such platforms, we found that bicrystalline silver nanowires exhibit a strong rate-dependent plastic deformation, as shown in Figure 3a. In addition, TEM images of the tested wires revealed that the dislocation density and distribution along the wire axis is dependent on the strain rate (see Figure 3b−d), which is consistent with stress relaxation kinetics under dynamic strain.[54] Our research shows that studies at higher strain rates will require the design and fabrication of novel systems to achieve high displacement speeds and control of electronic crosstalk during actuation and sensing.

Furthermore, simultaneous high-strain-rate deformation and imaging of nanostructures with atomic resolution presents a number of challenges. The highest strain rate attained with *in situ* TEM is 10^{-3}/s,[55] primarily due to the inability of the conventional TEM electron detectors to record events beyond ~35 frames/s.[10] As previously mentioned, the latest Cs/Cc-TEMs are capable of sub-angstrom resolution, but even state-of-the-art electron detectors with sufficient S/N ratio are capable of capturing only ~1600 frames/s.[28] In contrast, intermediate- and high-strain-rate experiments in few-micron-long samples, between 10^{-1}/s and 10^{5}, require electron detectors capable of capturing 1000−200 000 frames/s. Thus, with state-of-the-art electron detectors, it is only possible to capture the stress−strain signatures and the corresponding dynamic dislocation activities up to 10^{-1}/s strain rates.

Dynamic TEM (DTEM) offers an opportunity to overcome these limitations. The key difference between the DTEM in single-shot mode and the conventional TEM is the presence of more than 10^{6} electrons in the TEM column at any given time rather than a single electron.[56] In the pump−probe DTEM approach, a transient state is first attained in the material using an external stimulus, such as a laser pulse, and then examined using a pulse of electrons, triggered by a pulsed laser, at a specific time after the initiating event.[57,58] The spatial resolution of this technique is limited to the nanometer scale by electron−electron interactions and the brightness of the electron source. Hence, even with aberration corrections, sub-angstrom resolution would be still out of reach using DTEM.[59] Although temporal resolution in this method is in the nanosecond range, the span of the possible experiment is of a few microseconds, which means that the potentially interesting time scales for intermediate strain rates of nanomaterials (500 μs to 500 ms) are not attainable. A recent advance in DTEM to approach the microsecond time scale is the movie-mode DTEM (MM-DTEM), where the laser is used to generate serial electron pulses and a fast post-sample deflector is used to send each image to a separate region in the electron detector.[60] Currently, the minimum time between each frame is ~75 ns, providing capture rates >10 million frames/s with a maximum movie-mode duration of ~100 μs, which is ideal for experiments conducted with strain rates beyond 10^{4}/s. However, resolution continues to be a challenge (~100 nm) due to limitations in the electron source brightness.[59]

In order to explore high-strain-rate deformation of 1D materials and the kinetics of materials synthesis using *in situ* TEM, either faster electron detectors are required with the conventional TEM or the DTEM has to be modified to achieve longer movie-mode capture time periods. Currently, the challenge is to obtain high-speed complementary metal oxide semiconductor (CMOS)-based direct electron detectors with high quantum efficiency (DQE), which relates to the S/N ratio, and high modular transfer function, which measures the ability

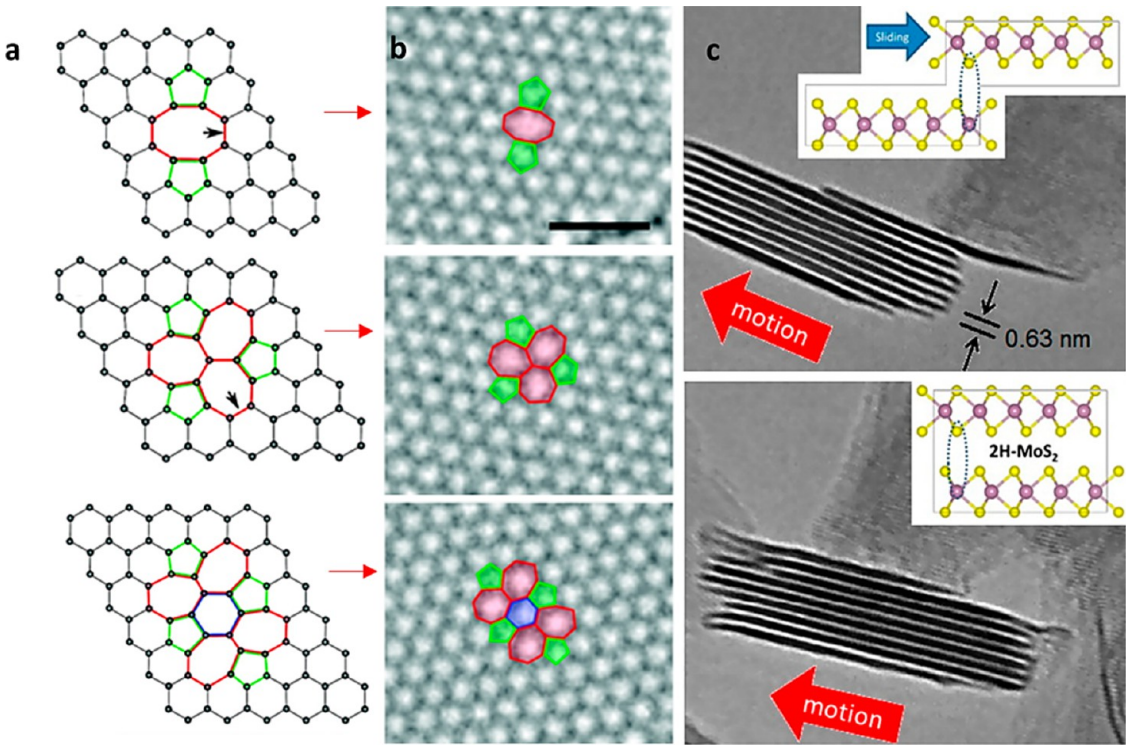

Figure 4. (a) Simulation of defects in graphene and (b) corresponding high-resolution TEM images. Reprinted from ref 77. Copyright 2010 American Chemical Society. (c) Interlayer sliding of MoS_2. Reprinted from ref 21. Copyright 2015 American Chemical Society.

of a detector to distinguish between a black−white transition.[61,62] Alternatively, the MM-DTEM can be further improved by increasing the source brightness using unconventional ultracold gas sources. Adding the ability to acquire millisecond-long movies and not limiting the total number of frames imposes challenges in detector multiplexing and computational challenges with throughput and storage.[63]

> One of the key limitations of *in situ* experiments of 2D materials is the difficulty in manipulating the sample from the growth substrate to the *in situ* TEM testing stage.

***In Situ* Transmission Electron Microscopy Applied to Two-Dimensional Materials.** In the past decade, one of the fastest growing research areas has been the property exploration of 2D material systems such as carbon-based 2D materials, including graphene and graphene oxide, and inorganic 2D materials, including hexagonal boron nitride and various chalcogenides, such as MoS_2.[64] Studies of analogues of graphene such as silicene, germanene, stanene, and phosphorene are also promising[65] due to their larger band gaps.[66] Indeed, silicene was recently used for the development of a single-layer field-effect transistor.[67] *In situ* TEM structural characterization of these 2D materials is particularly appealing, given that the lattice itself and lattice defects[68,69] can be observed using the ultrahigh spatial resolution of the Cs/Cc-TEM. In light of these advantages, a number of 2D materials have been imaged with *in situ* TEM to understand their structures.[70] However, *in situ* experiments have been primarily limited to understanding the effects of electron beam irradiation,[71,72] as shown in Figure 4b. Recently, reports have emerged on the effects of external stimuli, for example mechanical strain. Such experiments are important because shear and adhesive interactions are critical for leveraging the outstanding mechanical properties of 2D materials in macroscale nanocomposites. Recent examples include the study of crack propagation on graphene ribbons[73] and experiments probing interfacial interactions on MoS_2,[21] as shown in Figure 4c. In a recent *ACS Nano* report, Oviedo *et al.* performed detailed experiments with the *in situ* TEM in order to understand interlayer sliding in MoS_2. They observed how two layers slide against one another and determined the shear stress required to induce sliding within a large multilayer flake. This study proves that *in situ* TEM can also be used for interlayer nanotribology experiments in 2D materials.[21]

One of the key limitations of *in situ* experiments of 2D materials is the difficulty in manipulating the sample from the growth substrate to the *in situ* TEM testing stage. Some advances in specimen manipulation can pave the way to overcome

such challenges. For example, a recently reported novel way of fabricating Au thin nanobeam samples with a dog-bone-like shape using optical lithography makes manipulation of the specimen onto the stage less challenging.[74] Similarly, targeted growth of nanowires directly on MEMS tensile testing stages for *in situ* characterization has been demonstrated.[75] Analogous efforts for 2D materials could yield immense scientific insights, not only for mechanical properties but also in emerging phenomena, such as the piezoelectricity of MoS_2 and other chalcogenides.[76]

***In Situ* Transmission Electron Microscopy under Liquid Environments.** Liquid-stage TEM is an emerging *in situ* technique through which dynamic processes associated with nanoparticles, biological cells, lithium-based energy sources, *etc.* can be studied with high spatial and temporal resolutions.[12] Traditionally, due to the high vacuum requirement, TEM is incompatible with high-pressure liquids and therefore is used primarily for solid and dry samples.[19] To overcome this limitation, electron-beam-transparent silicon nitride (SiN) membranes were developed to enclose a small volume of liquid (called a liquid cell), thus isolating it from the microscope vacuum.[78] Liquid cell technology presents some challenges, such as difficulty in sealing, limitations in image resolution due to the thickness of the SiN window and the liquid layer, and unwanted crystal growth due to electron beam irradiation.[79] To address these challenges, improvements on this basic liquid cell design have emerged. Polymer O-rings are now used to seal the SiN windows instead of epoxy, thus improving the ease of fabrication and assembly.[80] Although the most commonly used liquid cells are enclosed with ~50 nm thick SiN windows, where the highest reported resolution is 2.1 Å,[32,79] enclosure of liquids has also been achieved by means of atomically thin membranes such as graphene.[29] In this case, the seal is provided by the van der Waals attraction between the graphene sheets. Although this technique increases the image resolution to 1 Å, the assembly of such graphene-based liquid cells is technically demanding, resulting in limited broad applicability.[12] Another problem stems from the knock-off damage threshold energy of graphene, which at 86 kV[71] leads to suboptimal resolution.[81]

The other major drawbacks in liquid cell technology arise mainly from the interactions of the electron beam with the liquid. These interactions result in radiolysis, creating radical species and aqueous electrons,[82] which can be both a problem and an advantage. These strongly-reducing species can react with electronegative ions from soluble transition metals to form crystals that can potentially lead to artifacts in images. By maintaining a constant flow through the liquid cell,[83] using the recently-developed continuous-flow *in situ* liquid stage,[84] and by the addition of electron-scavenging species such as dissolved oxygen and hydrogen peroxide to the liquid,[82] reactive species can be quenched before crystal formation.

In contrast, this radiolysis mechanism has been used advantageously for electron-beam-induced nanoparticle growth, shown in Figure 5a,b,e.[28,30,32,85,86] For example, using a 300 kV electron beam, platinum nanoparticles were grown from a 200 nm thick organic solution containing a platinum precursor while tracking the single-particle growth mechanisms.[28] The electron beam has also been used to control the growth mechanisms by attaching iron oxyhydroxide nanoparticles to one another, as shown in Figure 5c.[87] In order to understand the mechanism of nanoparticle nucleation and growth, high-speed imaging is required. For instance, the Pt nanoparticle growth micrograph shown in Figure 4a was taken using a Gatan K2-IS camera that can capture high-resolution electron images directly on a CMOS sensor at ~1600 frames/s. This camera is one of a new generation of electron detectors called "direct" electron detectors because they do not require scintillators or intermediate optical transfer of information from the high-voltage electrons to an electronic signal.

Other recent and important applications of liquid-stage *in situ* TEM are in the life sciences. Traditionally, imaging in the life sciences using a TEM has been conducted by cryo-TEM,[12] which freezes the sample and prohibits native motion, making the technique unsuitable for studying dynamic processes.[88] By using liquid cells, this problem has been circumvented. In fact, *in situ* TEM has been applied successfully to study soft organic materials and biological cells in real time to reveal their microscopic structures and dynamic processes.[32,88,89] Recently, live *E. coli* cells were imaged without structural damage by *in situ* TEM with a liquid cell, and the structure and dynamic movements of pili surrounding the *E. coli* cells were revealed.[89] There is little work being carried out in the field of live cell imaging *in situ* liquid TEM,[31,90] and even with state-of-the-art techniques, only nanometer resolution is attainable.

There are also issues that need to be addressed to track biological cells or other soft organic nanoparticle motion. These issues include agglomeration or repulsion of the particles due to beam-induced charging effects, which are pronounced after lengthy imaging, and the need for higher temporal resolution to monitor nanoparticles at the speed of Brownian motion (~28 μm/s) without compromising spatial resolution.[88]

In situ TEM with electrochemical liquid cells has also been used to study dynamic nanoscale processes like lithiation/delithiation, as shown in Figure 5d,[91] and electrode–electrolyte interactions in lithium ion batteries to elucidate the rechargeable capacity of the batteries and structural stability of the electrodes, respectively. In this

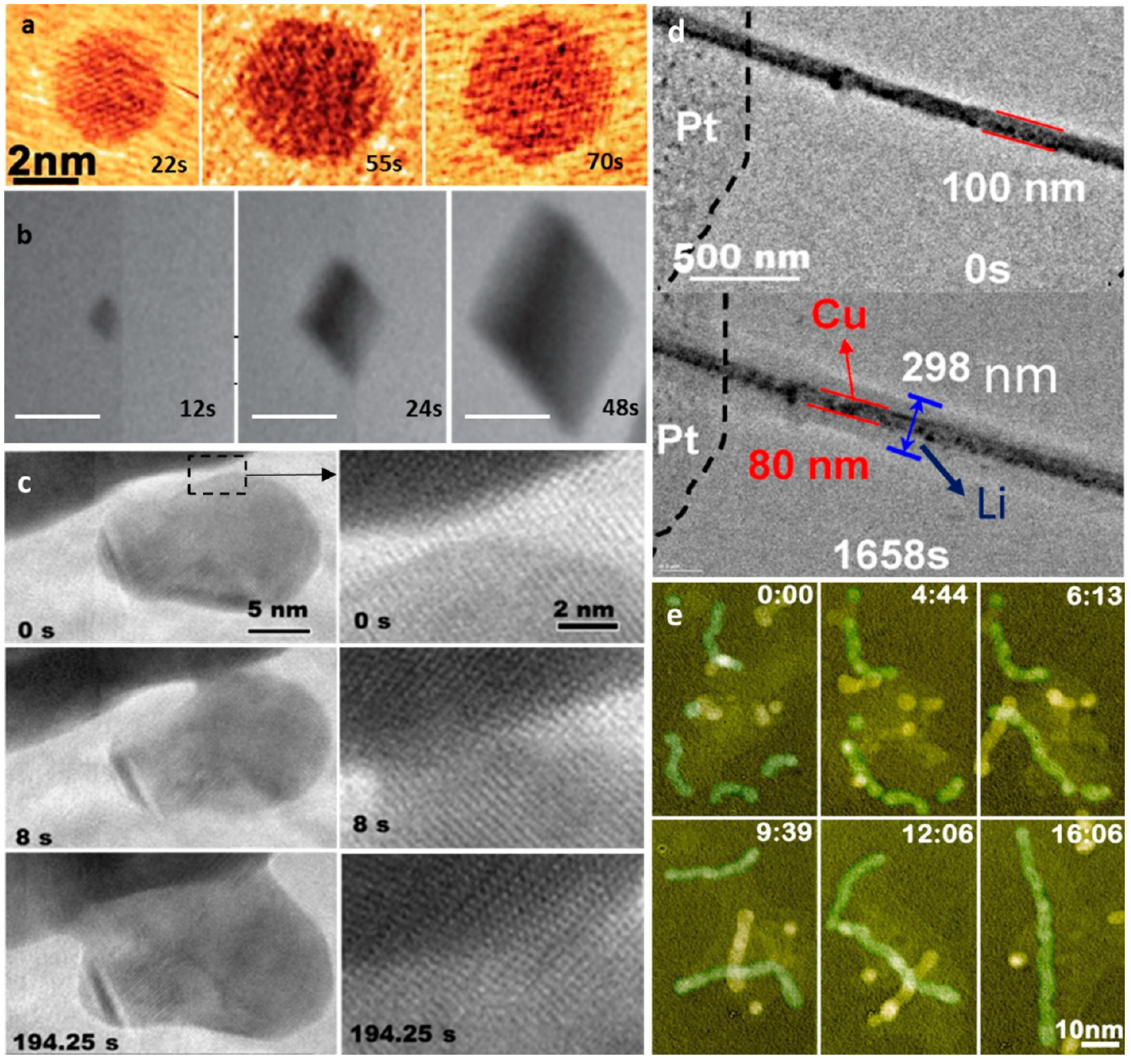

Figure 5. Examples of *in situ* liquid TEM. (a) Graphene-enclosed Pt nanoparticle growth captured using a GATAN K2-IS direct detection camera. Reprinted with permission from ref 28. Copyright 2014 American Association for the Advancement of Science. (b) Nucleation and growth of calcite crystals enclosed in SiN windows (scale bar 500 nm). Reprinted with permission from ref 86. Copyright 2014 American Association for the Advancement of Science. (c) Oriented attachment sequence of iron oxyhydroxide nanoparticles at low and high magnifications. Reprinted with permission from ref 87. Copyright 2012 American Association for the Advancement of Science. (d) Lithiation of a silicon nanowire in a liquid cell *in situ* TEM. Reprinted from ref 91. Copyright 2013 American Chemical Society. (e) Growth of Pt_3Fe nanorods. Reprinted with permission from ref 85. Copyright 2012 American Association for the Advancement of Science.

application, the limitation in spatial resolution arises from the thickness of the SiN windows, which prevents high-quality imaging of the atomic structure and its evolution in the solid electrode−electrolyte interface.[91] Some recent studies on silicon nanoparticles have been conducted with graphene windows, resulting in improved resolution.[33]

Future technical development of *in situ* TEM under liquid media primarily would involve improving the image resolution by enhancing the electron transparency of the liquid cell material and decreasing the thickness of the liquid layer *via* optimization of the spacer thickness between the windows of the liquid cell. Currently, the only alternative to SiN windows is graphene. Novel window materials that are more robust and tolerant to electron beam damage beyond 86 kV are needed for these studies to achieve their full potential. In that regard, further research needs to be conducted on the feasibility of using ~1 nm thick multilayer graphene windows (similar to the graphene sandwich approach[92]) instead of monolayers, or explore other 2D materials with potentially better performance under the electron beam.

In addition to the increase in spatial resolution, other improvements needed in the field of material nucleation, growth, and tracking include increases in temporal resolution with high-speed direct electron detectors capable of capturing more than 2000 frames/s. There is work underway to improve the S/N ratios in direct electron detectors, which are the main hurdles to faster capture rates.[62] In applications of nanomaterials to energy (*e.g.*, batteries),

interactions between electron beams and electrolytes at varying electron doses require better understanding.

CONCLUSIONS AND FUTURE OUTLOOK

In situ TEM is a versatile and powerful technique that helps reveal the dynamical behavior of nanoscale material systems in multiple spatial and temporal scales. Advanced TEM techniques have been increasingly employed but remain underutilized for *in situ* experiments. Perhaps this is because realizing the full potential of *in situ* TEM requires further advances in spatial and temporal resolution, along with stable *in situ* TEM experimental setups. Low spatial resolution in many *in situ* TEM techniques is primarily due to shortcomings of the *in situ* experimental setup rather than an intrinsic TEM limitation. In contrast, temporal resolution requires improvement to the TEM technology itself, such as a faster direct electron detector with adequate DQE or improved capability to capture images for time periods of milliseconds or more at high numbers of frames per second.

In situ TEM is a versatile and powerful technique that helps reveal the dynamical behavior of nanoscale material systems in multiple space and time scales.

Our review of the literature reveals that little work has been conducted with aberration correction microscopes in the area of mechanical and multiphysics (mechanical/thermal, thermal/electrical, *etc.*) testing of zero-dimensional (0D), 1D, and 2D nanomaterials. As work advances in this area, new challenges, particularly on the stability of setups, may become apparent. In particular, low-resonance-frequency *in situ* experimental setups may lead to unacceptable levels of mechanical noise, thus paving the way to more widespread commercially-available setups based on MEMS. However, even in these miniaturized setups, stability issues related to the size of the freestanding specimen, for example, its resonant frequencies and thermal noise, are expected to become important. Optimal design for increased thermal and mechanical stability, in addition to reduced specimen freestanding lengths (gage lengths) in the submicron regime, may become necessary.

In situ TEM will continue to revolutionize our atomic-level understanding of structure–function relationships in nanoscale materials.[93] Specifically, if electron detectors capable of capturing ~10 000–200 000 frames/s are built or DTEM is improved to record movies for longer time periods, capturing the kinetic behavior of nanostructures will become possible. A major breakthrough would be the direct comparison of atomistic simulation predictions and experimental results on comparable time scales, for example, through high-strain-rate testing of 1D and 2D nanomaterials and molecular modeling. In the area of *in situ* TEM under liquid environments, significant improvements in spatial resolution and radiation damage, through utilization of novel electron beam transparent materials and improved imaging conditions, could have a profound effect on understanding many biological processes such as single-cell transfection in the presence of electric fields[94] and dynamics of proteins, a key aspect to unlocking many biological mysteries such as Parkinson's and Alzheimer's disease.[95,96]

Conflict of Interest: The authors declare no competing financial interest.

Acknowledgment. This work is supported in part by a National Science Foundation grant [DMR-1408901], and Air Force Office of Scientific Research grant [FA9550-15-1-0009], and an Army Research Office grant [W911NF-15-1-0068].

REFERENCES AND NOTES

1. Knoll, M.; Ruska, E. Das Elektronenmikroskop. *Z. Phys.* **1932**, *78*, 318–339.
2. Williams, D. B.; Carter, C. B. *The Transmission Electron Microscope*; Springer: Berlin, 1996.
3. Jinschek, J. Advances in the Environmental Transmission Electron Microscope (ETEM) for Nanoscale *In Situ* Studies of Gas–Solid Interactions. *Chem. Commun.* **2014**, *50*, 2696–2706.
4. Kisielowski, C.; Freitag, B.; Bischoff, M.; Van Lin, H.; Lazar, S.; Knippels, G.; Tiemeijer, P.; van der Stam, M.; von Harrach, S.; Stekelenburg, M. Detection of Single Atoms and Buried Defects in Three Dimensions by Aberration-Corrected Electron Microscope with 0.5-Å Information Limit. *Microsc. Microanal.* **2008**, *14*, 469–477.
5. Dahmen, U.; Erni, R.; Radmilovic, V.; Ksielowski, C.; Rossell, M.-D.; Denes, P. Background, Status and Future of the Transmission Electron Aberration-Corrected Microscope Project. *Philos. Trans. R. Soc., A* **2009**, *367*, 3795–3808.
6. Schlossmacher, P.; Klenov, D. O.; Freitag, B.; von Harrach, S.; Steinbach, A. Nanoscale Chemical Compositional Analysis with an Innovative S/TEM-EDX System. *Microsc. Anal.* **2010**, *24*, S5–S8.
7. Freitag, B.; Knippels, G.; Kujawa, S.; Tiemeijer, P.; van der Stam, M.; Hubert, D.; Kisielowski, C.; Denes, P.; Minor, A.; Dahmen, U. In *First Performance Measurements and Application Results of a New High Brightness Schottky Field Emitter for HR-S/TEM at 80–300 kV Acceleration Voltage*; EMC 2008 14th European Microscopy Congress, September 1–5, 2008; Springer: Aachen, Germany, **2008**; pp 55–56.
8. Midgley, P. A.; Weyland, M.; Thomas, J. M.; Johnson, B. F. Z-Contrast Tomography: A Technique in Three-Dimensional Nanostructural Analysis Based on Rutherford Scattering. *Chem. Commun.* **2001**, 907–908 (see Supporting Information related to this article).
9. Kabius, B.; Hartel, P.; Haider, M.; Müller, H.; Uhlemann, S.; Loebau, U.; Zach, J.; Rose, H. First Application of Cc-Corrected Imaging for High-Resolution and Energy-Filtered TEM. *J. Electron Microsc.* **2009**, *58*, 147–155.
10. Espinosa, H. D.; Bernal, R. A.; Filleter, T. *In Situ* TEM Electromechanical Testing of Nanowires and Nanotubes. *Small* **2012**, *8*, 3233–3252.
11. Zhang, M.; Olson, E.; Twesten, R.; Wen, J.; Allen, L.; Robertson, I.; Petrov, I. *In Situ* Transmission Electron Microscopy Studies Enabled by Microelectromechanical System Technology. *J. Mater. Res.* **2005**, *20*, 1802–1807.
12. Chen, X.; Li, C.; Cao, H. Recent Developments of *In Situ* Wet Cell Technology for Transmission Electron

Microscopies. *Nanoscale* **2015**, *7*, 4811–4819.
13. Yu, Q.; Legros, M.; Minor, A. *In Situ* TEM Nanomechanics. *MRS Bull.* **2015**, *40*, 62–70.
14. Zhu, Y.; Espinosa, H. D. An Electromechanical Material Testing System for *In Situ* Electron Microscopy and Applications. *Proc. Natl. Acad. Sci. U.S.A.* **2005**, *102*, 14503–14508.
15. Bernal, R. A.; Filleter, T.; Connell, J. G.; Sohn, K.; Huang, J.; Lauhon, L. J.; Espinosa, H. D. *In Situ* Electron Microscopy Four-Point Electromechanical Characterization of Freestanding Metallic and Semiconducting Nanowires. *Small* **2014**, *10*, 725–733.
16. Shan, Z.; Adesso, G.; Cabot, A.; Sherburne, M.; Asif, S. S.; Warren, O.; Chrzan, D.; Minor, A.; Alivisatos, A. Ultrahigh Stress and Strain in Hierarchically Structured Hollow Nanoparticles. *Nat. Mater.* **2008**, *7*, 947–952.
17. Peng, B.; Locascio, M.; Zapol, P.; Li, S.; Mielke, S. L.; Schatz, G. C.; Espinosa, H. D. Measurements of Near-Ultimate Strength for Multiwalled Carbon Nanotubes and Irradiation-Induced Crosslinking Improvements. *Nat. Nanotechnol.* **2008**, *3*, 626–631.
18. Bernal, R. A.; Agrawal, R.; Peng, B.; Bertness, K. A.; Sanford, N. A.; Davydov, A. V.; Espinosa, H. D. Effect of Growth Orientation and Diameter on the Elasticity of GaN Nanowires. A Combined *In Situ* TEM and Atomistic Modeling Investigation. *Nano Lett.* **2011**, *11*, 548–555.
19. Wang, C.-M.; Liao, H.-G.; Ross, F. M. Observation of Materials Processes in Liquids by Electron Microscopy. *MRS Bull.* **2015**, *40*, 46–52.
20. Warner, J. H.; Margine, E. R.; Mukai, M.; Robertson, A. W.; Giustino, F.; Kirkland, A. I. Dislocation-Driven Deformations in Graphene. *Science* **2012**, *337*, 209–212.
21. Oviedo, J. P.; KC, S.; Lu, N.; Wang, J.; Cho, K.; Wallace, R. M.; Kim, M. J. *In Situ* TEM Characterization of Shear-Stress-Induced Interlayer Sliding in the Cross Section View of Molybdenum Disulfide. *ACS Nano* **2015**, *9*, 1543–1551.
22. Filleter, T.; Ryu, S.; Kang, K.; Yin, J.; Bernal, R. A.; Sohn, K.; Li, S.; Huang, J.; Cai, W.; Espinosa, H. D. Nucleation-Controlled Distributed Plasticity in Penta-Twinned Silver Nanowires. *Small* **2012**, *8*, 2986–2993.
23. Bernal, R. A.; Aghaei, A.; Lee, S.; Ryu, S.; Sohn, K.; Huang, J.; Cai, W.; Espinosa, H. Intrinsic Bauschinger Effect and Recoverable Plasticity in Pentatwinned Silver Nanowires Tested in Tension. *Nano Lett.* **2015**, *15*, 139–146.
24. Kiener, D.; Minor, A. Source Truncation and Exhaustion: Insights from Quantitative *In Situ* TEM Tensile Testing. *Nano Lett.* **2011**, *11*, 3816–3820.
25. Zheng, K.; Wang, C.; Cheng, Y.-Q.; Yue, Y.; Han, X.; Zhang, Z.; Shan, Z.; Mao, S. X.; Ye, M.; Yin, Y. Electron-Beam-Assisted Superplastic Shaping of Nanoscale Amorphous Silica. *Nat. Commun.* **2010**, *1*, 24.
26. Zheng, H.; Cao, A.; Weinberger, C. R.; Huang, J. Y.; Du, K.; Wang, J.; Ma, Y.; Xia, Y.; Mao, S. X. Discrete Plasticity in Sub-10-nm-Sized Gold Crystals. *Nat. Commun.* **2010**, *1*, 144.
27. Liao, H.-G.; Zheng, H. Liquid Cell Transmission Electron Microscopy Study of Platinum Iron Nanocrystal Growth and Shape Evolution. *J. Am. Chem. Soc.* **2013**, *135*, 5038–5043.
28. Liao, H.-G.; Zherebetskyy, D.; Xin, H.; Czarnik, C.; Ercius, P.; Elmlund, H.; Pan, M.; Wang, L.-W.; Zheng, H. Facet Development During Platinum Nanocube Growth. *Science* **2014**, *345*, 916–919.
29. Yuk, J. M.; Park, J.; Ercius, P.; Kim, K.; Hellebusch, D. J.; Crommie, M. F.; Lee, J. Y.; Zettl, A.; Alivisatos, A. P. High-Resolution EM of Colloidal Nanocrystal Growth Using Graphene Liquid Cells. *Science* **2012**, *336*, 61–64.
30. Zheng, H.; Smith, R. K.; Jun, Y.-w.; Kisielowski, C.; Dahmen, U.; Alivisatos, A. P. Observation of Single Colloidal Platinum Nanocrystal Growth Trajectories. *Science* **2009**, *324*, 1309–1312.
31. Peckys, D. B.; Mazur, P.; Gould, K. L.; de Jonge, N. Fully Hydrated Yeast Cells Imaged with Electron Microscopy. *Biophys. J.* **2011**, *100*, 2522–2529.
32. Evans, J. E.; Jungjohann, K. L.; Browning, N. D.; Arslan, I. Controlled Growth of Nanoparticles from Solution with *In Situ* Liquid Transmission Electron Microscopy. *Nano Lett.* **2011**, *11*, 2809–2813.
33. Luo, L.; Wu, J.; Luo, J.; Huang, J.; Dravid, V. P. Dynamics of Electrochemical Lithiation/Delithiation of Graphene-Encapsulated Silicon Nanoparticles Studied by *In-Situ* TEM. *Sci. Rep.* **2014**, *4*, 3863.
34. Warner, J. H.; Rümmeli, M. H.; Ge, L.; Gemming, T.; Montanari, B.; Harrison, N. M.; Büchner, B.; Briggs, G. A. D. Structural Transformations in Graphene Studied with High Spatial and Temporal Resolution. *Nat. Nanotechnol.* **2009**, *4*, 500–504.
35. Erickson, K.; Erni, R.; Lee, Z.; Alem, N.; Gannett, W.; Zettl, A. Determination of the Local Chemical Structure of Graphene Oxide and Reduced Graphene Oxide. *Adv. Mater.* **2010**, *22*, 4467–4472.
36. Husain, A.; Hone, J.; Postma, H. W. C.; Huang, X.; Drake, T.; Barbic, M.; Scherer, A.; Roukes, M. Nanowire-Based Very-High-Frequency Electromechanical Resonator. *Appl. Phys. Lett.* **2003**, *83*, 1240–1242.
37. Loh, O. Y.; Espinosa, H. D. Nanoelectromechanical Contact Switches. *Nat. Nanotechnol.* **2012**, *7*, 283–295.
38. Hu, L.; Kim, H. S.; Lee, J.-Y.; Peumans, P.; Cui, Y. Scalable Coating and Properties of Transparent, Flexible, Silver Nanowire Electrodes. *ACS Nano* **2010**, *4*, 2955–2963.
39. Espinosa, H. D.; Bernal, R. A.; Minary-Jolandan, M. A. Review of Mechanical and Electromechanical Properties of Piezoelectric Nanowires. *Adv. Mater.* **2012**, *24*, 4656–4675.
40. Shan, Z.; Mishra, R. K.; Asif, S. S.; Warren, O. L.; Minor, A. M. Mechanical Annealing and Source-Limited Deformation in Submicrometre-Diameter Ni Crystals. *Nat. Mater.* **2008**, *7*, 115–119.
41. Zheng, H.; Meng, Y. S.; Zhu, Y. Frontiers of *In Situ* Electron Microscopy. *MRS Bull.* **2015**, *40*, 12–18.
42. Filleter, T.; Bernal, R.; Li, S.; Espinosa, H. Ultrahigh Strength and Stiffness in Cross-Linked Hierarchical Carbon Nanotube Bundles. *Adv. Mater.* **2011**, *23*, 2855–2860.
43. Liu, L.; Wang, J.; Gong, S.; Mao, S. Atomistic Observation of a Crack Tip Approaching Coherent Twin Boundaries. *Sci. Rep.* **2014**, *4*, 4397.
44. Pantano, M. F.; Bernal, R. A.; Pagnotta, L.; Espinosa, H. D. Multiphysics Design and Implementation of a Microsystem for Displacement-Controlled Tensile Testing of Nanomaterials. *Meccanica* **2015**, *50*, 549–560.
45. Qin, Q.; Yin, S.; Cheng, G.; Li, X.; Chang, T.-H.; Richter, G.; Zhu, Y.; Gao, H. Recoverable Plasticity in Penta-twinned Metallic Nanowires Governed by Dislocation Nucleation and Retraction. *Nat. Commun.* **2015**, *6*, 5983.
46. Ensslen, C.; Kraft, O.; Mönig, R.; Xu, J.; Zhang, G.-P.; Schneider, R. Mechanical Annealing of Cu–Si Nanowires during High-Cycle Fatigue. *MRS Commun.* **2014**, *4*, 83–87.
47. Li, P.; Liao, Q.; Yang, S.; Bai, X.; Huang, Y.; Yan, X.; Zhang, Z.; Liu, S.; Lin, P.; Kang, Z. *In Situ* Transmission Electron Microscopy Investigation on Fatigue Behavior of Single ZnO Wires under High-Cycle Strain. *Nano Lett.* **2014**, *14*, 480–485.
48. Lee, S.; Im, J.; Yoo, Y.; Bitzek, E.; Kiener, D.; Richter, G.; Kim, B.; Oh, S. H. Reversible Cyclic Deformation Mechanism of Gold Nanowires by Twinning–Detwinning Transition Evidenced from *In Situ* TEM. *Nat. Commun.* **2014**, *5*, 3033.
49. Rajagopalan, J.; Rentenberger, C.; Karnthaler, H. P.; Dehm, G.; Saif, M. T. A. *In Situ* TEM Study of Microplasticity and Bauschinger Effect in Nanocrystalline Metals. *Acta Mater.* **2010**, *58*, 4772–4782.
50. Weinberger, C. R.; Jennings, A. T.; Kang, K.; Greer, J. R. Atomistic Simulations and Continuum Modeling of Dislocation Nucleation and Strength in Gold Nanowires. *J. Mech. Phys. Solids* **2012**, *60*, 84–103.
51. Clifton, R. High Strain Rate Behavior of Metals. *Appl. Mech. Rev.* **1990**, *43*, S9–S22.
52. Espinosa, H. D.; Nemat-Nasser, S. Low-Velocity Impact Testing. In *ASM Handbook: Mechanical Testing*

and Evaluation; Kuhn, H., Medlin, D., Eds.; ASM International: Materials Park, OH, 2000; Vol. 8, pp 539−559.
53. Elgamel, M. A.; Bayoumi, M. A. Cross-talk Noise Analysis in Ultra Deep Submicrometer Technologies. *Interconnect Noise Optimization in Nanometer Technologies*; Springer: New York, 2006; pp 45−57.
54. Ramachandramoorthy, R.; Gao, W.; Bernal, R. A.; Espinosa, H. Brittle-to-ductile transition in bicrystalline silver nanowires revealed by high strain rate tensile testing. Manuscript in preparation.
55. Oh, S. H.; Legros, M.; Kiener, D.; Dehm, G. *In Situ* Observation of Dislocation Nucleation and Escape in a Submicrometre Aluminium Single Crystal. *Nat. Mater.* **2009**, *8*, 95–100.
56. LaGrange, T.; Armstrong, M.; Boyden, K.; Brown, C.; Campbell, G.; Colvin, J.; DeHope, W.; Frank, A.; Gibson, D.; Hartemann, F. Single-Shot Dynamic Transmission Electron Microscopy. *Appl. Phys. Lett.* **2006**, *89*, 044105.
57. Armstrong, M. R.; Boyden, K.; Browning, N. D.; Campbell, G. H.; Colvin, J. D.; DeHope, W. J.; Frank, A. M.; Gibson, D. J.; Hartemann, F.; Kim, J. S. Practical Considerations for High Spatial and Temporal Resolution Dynamic Transmission Electron Microscopy. *Ultramicroscopy* **2007**, *107*, 356–367.
58. LaGrange, T.; Campbell, G. H.; Reed, B.; Taheri, M.; Pesavento, J. B.; Kim, J. S.; Browning, N. D. Nanosecond Time-Resolved Investigations Using the *In Situ* of Dynamic Transmission Electron Microscope (DTEM). *Ultramicroscopy* **2008**, *108*, 1441–1449.
59. LaGrange, T.; Reed, B. W.; Masiel, D. J. Movie-Mode Dynamic Electron Microscopy. *MRS Bull.* **2015**, *40*, 22–28.
60. LaGrange, T.; Reed, B.; McKeown, J.; Santala, M.; Dehope, W.; Huete, G.; Shuttlesworth, R.; Campbell, G. Movie Mode Dynamic Transmission Electron Microscope: Revealing Material Processes at Nanometer and Nanosecond Scales with Multiframe Acquisition. *Microsc. Microanal.* **2013**, *19*, 1154–1155.
61. Ziegler, A.; Graafsma, H.; Zhang, X. F.; Frenken, J. W. *In-Situ Materials Characterization: Across Spatial and Temporal Scales*; Springer Science & Business Media: Berlin, 2014; Vol. 193.
62. Krieger, B.; Contarato, D.; Denes, P.; Doering, D.; Gnani, D.; Joseph, J.; Schindler, S. *Fast, Radiation Hard, Direct Detection CMOS Imagers for High Resolution Transmission Electron Microscopy*; Nuclear Science Symposium and Medical Imaging Conference (NSS/MIC), October 23−29, **2011**, IEEE; pp 1946−1949.
63. Reed, B.; Armstrong, M.; Browning, N.; Campbell, G.; Evans, J.; LaGrange, T.; Masiel, D. The Evolution of Ultrafast Electron Microscope Instrumentation. *Microsc. Microanal.* **2009**, *15*, 272–281.
64. Sun, L.; Banhart, F.; Warner, J. Two-Dimensional Materials under Electron Irradiation. *MRS Bull.* **2015**, *40*, 29–37.
65. Balendhran, S.; Walia, S.; Nili, H.; Sriram, S.; Bhaskaran, M. Elemental Analogues of Graphene: Silicene, Germanene, Stanene, and Phosphorene. *Small* **2014**, *6*, 640–652.
66. Reich, E. S. Phosphorene Excites Materials Scientists. *Nature* **2014**, *506*, 19.
67. Tao, L.; Cinquanta, E.; Chiappe, D.; Grazianetti, C.; Fanciulli, M.; Dubey, M.; Molle, A.; Akinwande, D. Silicene Field-Effect Transistors Operating at Room Temperature. *Nat. Nanotechnol.* **2015**, *10*, 227–231.
68. Liu, X.; Xu, T.; Wu, X.; Zhang, Z.; Yu, J.; Qiu, H.; Hong, J.-H.; Jin, C.-H.; Li, J.-X.; Wang, X.-R. Top-Down Fabrication of Sub-nanometre Semiconducting Nanoribbons Derived from Molybdenum Disulfide Sheets. *Nat. Commun.* **2013**, *4*, 1776.
69. Qiu, H.; Xu, T.; Wang, Z.; Ren, W.; Nan, H.; Ni, Z.; Chen, Q.; Yuan, S.; Miao, F.; Song, F. Hopping Transport through Defect-Induced Localized States in Molybdenum Disulphide. *Nat. Commun.* **2013**, *4*, 2642.
70. Robertson, A. W.; Montanari, B.; He, K.; Allen, C. S.; Wu, Y. A.; Harrison, N. M.; Kirkland, A. I.; Warner, J. H. Structural Reconstruction of the Graphene Monovacancy. *ACS Nano* **2013**, *7*, 4495–4502.
71. Robertson, A. W.; Allen, C. S.; Wu, Y. A.; He, K.; Olivier, J.; Neethling, J.; Kirkland, A. I.; Warner, J. H. Spatial Control of Defect Creation in Graphene at the Nanoscale. *Nat. Commun.* **2012**, *3*, 1144.
72. Rong, Y.; Warner, J. H. Wired Up: Interconnecting Two-Dimensional Materials with One-Dimensional Atomic Chains. *ACS Nano* **2014**, *8*, 11907–11912.
73. Zhang, P.; Ma, L.; Fan, F.; Zeng, Z.; Peng, C.; Loya, P. E.; Liu, Z.; Gong, Y.; Zhang, J.; Zhang, X. Fracture Toughness of Graphene. *Nat. Commun.* **2014**, *5*, 3782.
74. Hosseinian, E.; Pierron, O. N. Quantitative *In Situ* TEM Tensile Fatigue Testing on Nanocrystalline Metallic Ultrathin Films. *Nanoscale* **2013**, *5*, 12532–12541.
75. Wagesreither, S.; Bertagnolli, E.; Kawase, S.; Isono, Y.; Lugstein, A. Electrostatic Actuated Strain Engineering in Monolithically Integrated VLS Grown Silicon Nanowires. *Nanotechnology* **2014**, *25*, 455705.
76. Wu, W.; Wang, L.; Li, Y.; Zhang, F.; Lin, L.; Niu, S.; Chenet, D.; Zhang, X.; Hao, Y.; Heinz, T. F. Piezoelectricity of Single-Atomic-Layer MoS_2 for Energy Conversion and Piezotronics. *Nature* **2014**, *514*, 470–474.
77. Banhart, F.; Kotakoski, J.; Krasheninnikov, A. V. Structural Defects in Graphene. *ACS Nano* **2010**, *5*, 26–41.
78. Williamson, M.; Tromp, R.; Vereecken, P.; Hull, R.; Ross, F. Dynamic Microscopy of Nanoscale Cluster Growth at the Solid−Liquid Interface. *Nat. Mater.* **2003**, *2*, 532–536.
79. Woehl, T. J.; Jungjohann, K. L.; Evans, J. E.; Arslan, I.; Ristenpart, W. D.; Browning, N. D. Experimental Procedures To Mitigate Electron Beam Induced Artifacts during *In Situ* Fluid Imaging of Nanomaterials. *Ultramicroscopy* **2013**, *127*, 53–63.
80. Franks, R.; Morefield, S.; Wen, J.; Liao, D.; Alvarado, J.; Strano, M.; Marsh, C. A Study of Nanomaterial Dispersion in Solution by Wet-Cell Transmission Electron Microscopy. *J. Nanosci. Nanotechnol.* **2008**, *8*, 4404–4407.
81. Stöger-Pollach, M.; Pongratz, P. Advantages of Low Beam Energies in a TEM for Valence EELS. *J. Phys.: Conf. Ser.* **2010**, 012031.
82. Hart, E. J. The Hydrated Electron. *Science* **1964**, *146*, 1664–1664.
83. De Jonge, N.; Peckys, D. B.; Kremers, G.; Piston, D. Electron Microscopy of Whole Cells in Liquid with Nanometer Resolution. *Proc. Natl. Acad. Sci. U.S.A* **2009**, *106*, 2159–2164.
84. Klein, K.; Anderson, I.; De Jonge, N. Transmission Electron Microscopy with a Liquid Flow Cell. *J. Microsc.* **2011**, *242*, 117–123.
85. Liao, H.-G.; Cui, L.; Whitelam, S.; Zheng, H. Real-Time Imaging of Pt_3Fe Nanorod Growth in Solution. *Science* **2012**, *336*, 1011–1014.
86. Nielsen, M. H.; Aloni, S.; De Yoreo, J. J. *In Situ* TEM Imaging of $CaCO_3$ Nucleation Reveals Coexistence of Direct and Indirect Pathways. *Science* **2014**, *345*, 1158–1162.
87. Li, D.; Nielsen, M. H.; Lee, J. R.; Frandsen, C.; Banfield, J. F.; De Yoreo, J. J. Direction-Specific Interactions Control Crystal Growth by Oriented Attachment. *Science* **2012**, *336*, 1014–1018.
88. Proetto, M. T.; Rush, A. M.; Chien, M.-P.; Abellan Baeza, P.; Patterson, J. P.; Thompson, M. P.; Olson, N. H.; Moore, C. E.; Rheingold, A. L.; Andolina, C. Dynamics of Soft Nanomaterials Captured by Transmission Electron Microscopy in Liquid Water. *J. Am. Chem. Soc.* **2014**, *136*, 1162–1165.
89. Wang, Y.; Chen, X.; Cao, H.; Deng, C.; Cao, X.; Wang, P. A Structural Study of *Escherichia coli* Cells Using an *In Situ* Liquid Chamber TEM Technology. *J. Anal. Meth. Chem.* **2015**, 829302.
90. Liu, K.-L.; Wu, C.-C.; Huang, Y.-J.; Peng, H.-L.; Chang, H.-Y.; Chang, P.; Hsu, L.; Yew, T.-R. Novel Microchip for *In Situ* TEM Imaging of Living Organisms and Bio-reactions in Aqueous Conditions. *Lab Chip* **2008**, *8*, 1915–1921.
91. Gu, M.; Parent, L. R.; Mehdi, B. L.; Unocic, R. R.; McDowell, M. T.; Sacci, R. L.; Xu, W.; Connell, J. G.; Xu, P.; Abellan, P. Demonstration of an Electrochemical Liquid Cell for Operando Transmission Electron Microscopy Observation of the

Lithiation/Delithiation Behavior of Si Nanowire Battery Anodes. *Nano Lett.* **2013**, *13*, 6106–6112.
92. Algara-Siller, G.; Kurasch, S.; Sedighi, M.; Lehtinen, O.; Kaiser, U. The Pristine Atomic Structure of MoS_2 Monolayer Protected from Electron Radiation Damage by Graphene. *Appl. Phys. Lett.* **2013**, *103*, 203107.
93. Future of Electron Scattering and Diffraction. http://science.energy.gov/~/media/bes/pdf/reports/files/Future_of_Electron_Scattering.pdf.
94. Kang, W.; Yavari, F.; Minary-Jolandan, M.; Giraldo-Vela, J. P.; Safi, A.; McNaughton, R. L.; Parpoil, V.; Espinosa, H. D. Nanofountain Probe Electroporation (NFP-E) of Single Cells. *Nano Lett.* **2013**, *13*, 2448–2457.
95. Avila, J.; Lucas, J. J.; Perez, M.; Hernandez, F. Role of Tau Protein in Both Physiological and Pathological Conditions. *Physiol. Rev.* **2004**, *84*, 361–384.
96. Lippincott-Schwartz, J.; Manley, S. Putting Super-Resolution Fluorescence Microscopy To Work. *Nat. Methods* **2009**, *6*, 21–23.